NRL Memorandum Report 4689

Level Shifts and Inelastic Electron Scattering in Dense Plasmas

J. DAVIS

Plasma Radiation Group
Plasma Physics Division

M. BLAHA

Laboratory for Plasma and Fusion Energy Studies
University of Maryland
College Park, Maryland 20742

December 10, 1981

NAVAL RESEARCH LABORATORY
Washington, D.C.

SECURITY CLASSIFICATION OF THIS PAGE (When Data Entered)

REPORT DOCUMENTATION PAGE		READ INSTRUCTIONS BEFORE COMPLETING FORM
1. REPORT NUMBER NRL Memorandum Report 4689	2. GOVT ACCESSION NO. AD-A108 799	3. RECIPIENT'S CATALOG NUMBER
4. TITLE (and Subtitle) LEVEL SHIFTS AND INELASTIC ELECTRON SCATTERING IN DENSE PLASMAS		5. TYPE OF REPORT & PERIOD COVERED Interim report on a continuing NRL problem. 6. PERFORMING ORG. REPORT NUMBER
7. AUTHOR(s) J. Davis and M. Blaha*		8. CONTRACT OR GRANT NUMBER(s)
9. PERFORMING ORGANIZATION NAME AND ADDRESS Naval Research Laboratory Washington, DC 20375		10. PROGRAM ELEMENT, PROJECT, TASK AREA & WORK UNIT NUMBERS 61153N; RR011-09-41; 47-0911-02
11. CONTROLLING OFFICE NAME AND ADDRESS Office of Naval Research Arlington, VA 22217		12. REPORT DATE December 10, 1981 13. NUMBER OF PAGES 34
14. MONITORING AGENCY NAME & ADDRESS(if different from Controlling Office)		15. SECURITY CLASS. (of this report) UNCLASSIFIED 15a. DECLASSIFICATION/DOWNGRADING SCHEDULE

16. DISTRIBUTION STATEMENT (of this Report)

Approved for public release; distribution unlimited.

17. DISTRIBUTION STATEMENT (of the abstract entered in Block 20, if different from Report)

18. SUPPLEMENTARY NOTES

*Present address: Laboratory for Plasma and Fusion Energy Studies, University of Maryland, College Park, MD 20742.

19. KEY WORDS (Continue on reverse side if necessary and identify by block number)

Dense plasmas
Atomic processes
Electron scattering
Level shifts
Neon
Argon

20. ABSTRACT (Continue on reverse side if necessary and identify by block number)

A completely quantum mechanical formalism has been developed to describe the high density plasma effects on fundamental atomic parameters. Both the bound and free electrons are treated by a method which in principle is similar to Hartree's self-consistent field method. The free plasma electrons' wave-function is obtained from the Schrödinger equation with the effective potential representing the spherically averaged Coulomb interaction with bound and free electrons. Results are given for level shifts, coefficients of

(Continues)

DD FORM 1 JAN 73 1473 EDITION OF 1 NOV 65 IS OBSOLETE
S/N 0102-014-6601

SECURITY CLASSIFICATION OF THIS PAGE (When Data Entered)

20. ABSTRACT (Continued)

transition probabilities, and electron collision cross sections of Ne^{+9} for temperature and 200 and 500 eV for an electron density range of 1 - 6 X 10^{24} cm^{-3}, and of Ar^{+17} for temperatures of 1000 and 2000 eV and electron densities from 2 X 10^{25} to 8 X 10^{25} cm^{-3}. In the low-density region, level shifts are obtained for H and He^{+}.

CONTENTS

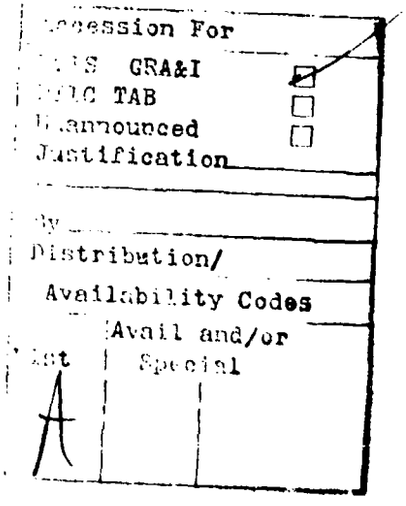

LEVEL SHIFTS AND INELASTIC ELECTRON SCATTERING IN DENSE PLASMAS

I. INTRODUCTION

The plasma polarization shift of spectral lines remains a basic and controversial effect. Griem[1] tried to explain the blue shifts for the resonance lines of ionized helium by considering the perturbation of the upper levels by free plasma electrons. An alternate approach involves the solution of the Schrödinger equation for the bound electrons in the Debye-Hückel potential. This leads to red shifts of the lines because it causes large shifts of the lower levels. Experimentally, evidence has been reported for blue shifts[2] of Lyman lines and red shifts[3] for Balmer lines for He II, but shifts measured for other similar ionized emitters are much smaller or zero.

Theimer and Kepple[4] have shown that the theory using the Debye-Hückel potential is inadequate because it ignores the reaction of plasma electrons to the presence of the bound electron. Their self-consistent calculation for a hydrogen plasma indicates much smaller level shifts than those predicted by previous theories. More recently, an analogous treatment was adopted by Rozsnyai[5] and Skupsky[6] with similar results. In these theories the free electron gas was treated classically and the energy levels were obtained from the solution of the Schrödinger equation.

In the present investigation we obtained level shifts, transition probability coefficients and collision cross sections for Ne^{+9} and Ar^{+17} in a plasma with electron density ranging from 10^{24} to 6×10^{24} cm^{-3} (for Ne^{+9}) and from 2×10^{25} to 8×10^{25} cm^{-3} (for Ar^{+17}) using a quantum-mechanical description of the plasma electrons. The theory in a simplified form was applied to the low-density region and level shifts were obtained for H and He^{+}.

II. DESCRIPTION OF THE METHOD

We consider an isolated impurity ion with nuclear charge Z immersed in a fully ionized hydrogen plasma. For simplicity all electric charges are assumed to have a spherically symmetric charge distribution. In addition, the positive charge due to protons is continuously distributed. This last assumption is probably the most drastic simplification that we have adopted.

Manuscript submitted October 6, 1981.

Two types of ions will be studied: completely stripped ions and one-electron hydrogenic ions. In the latter case, it is assumed that in a dense hot plasma the average local charge density due to the bound electron can be written as (atomic units are used throughout the paper, unless indicated)

$$\rho_b = - (4\pi r^2)^{-1} \sum_{n\ell} b_{n\ell} P^2_{n\ell} (r), \tag{1}$$

where $b_{n\ell}$ are the occupation numbers, $P_{n\ell}(r)$ are normalized radial wave functions, and $\sum_{n\ell} b_{n\ell} = 1$. In order for this assumption to be valid it is necessary that the average time between collisions leading to ionization and recombination be substantially larger than the time between collisions that change the state of excitation. Generally, the occupation numbers represent an average state of excitation of the ion and are determined by all possible collisional and radiative processes involving the bound electron. Due to the complexity of this situation, simplifying assumptions about $b_{n\ell}$ will be adopted.

If ρ_e and ρ_p represent local charge densities due to the free electrons and protons, the electrostatic potential V(r) at the distance r from the nucleus with charge Z is then given by

$$V(r) = Z r^{-1} + 4\pi \left[r^{-1} \int_0^r r^2 (\rho_e + \rho_p + \rho_b)\, dr + \int_r^\infty r (\rho_e + \rho_p + \rho_b)\, dr \right]. \tag{2}$$

At large distances from the ion, $\rho_b = 0$ and the plasma is neutral, so that

$$- \rho_e = \rho_p \equiv \rho_\infty \equiv N_e. \tag{3}$$

The positive charge distribution is described by classical Boltzmann statistics, viz.

$$\rho_p = \rho_\infty \exp (-V/k_B T), \tag{4}$$

where V(r) is given by (2), T is the temperature and k_B the Boltzmann constant.

The free electrons are represented by a Fermi-Dirac energy distribuiton outside a spherical boundary corresponding to the distance r_o from the nucleus; however, inside this boundary they can be treated quantum-mechanically and described by wave functions which are solutions of the time independent Schrodinger equation. In practical calculations the distance r_o is taken to be large enough so that plasma at the boundary may be considered neutral and condition (3) valid within numerical accuracy. The wave functions for the free electrons with energy $\frac{1}{2}k^2$ at $r > r_o$ can be expanded in partial waves and the expression for the spherically averaged charge density due to the free electrons at any r is then given by

$$\rho_e = - \int_0^\infty W(k)\ (kr^2)^{-1} \sum_{\ell=0}^{\infty} (2\ell+1)\ F_{k\ell}^2\ (r)\ dk, \tag{5}$$

where

$$W(k) = \pi^{-2}k^2 \left[1 + \exp\left\{(\tfrac{1}{2}k^2 - \mu)/k_B T\right\}\right]^{-1}. \tag{6}$$

μ is the chemical potential of the free electron gas determined by the condition

$$\int_0^\infty W(k)\ dk = \rho_\infty \tag{7}$$

and the functions $F_{k\ell}$ are solutions of the equation

$$\left[\frac{d^2}{dr^2} - \frac{\ell(\ell+1)}{r^2} + 2V(r) - 2V_{ex}(r) - 2V_{corr}(r) + 2V_{ex}(\infty) + 2V_{corr}(\infty) + k^2\right] F_{k\ell}(r) = 0 \tag{8}$$

with the asymptotic form

$$F_{k\ell}(r) \sim k^{-\frac{1}{2}} \sin\ (kr + \delta_{k\ell}). \tag{9}$$

The electrostatic potential V is given by (2) and the exchange energy V_{ex} and the correlation energy V_{corr} of a free electron in a plasma were taken from Dharma-wardana[7,8] and Taylor[8] and are given in terms of temperature T and local electron density $N_e \equiv = \rho_e$:

$$V_{ex} = -0.4073\, r_s^{-1} \tanh(\tau^{-1}), \tag{10}$$

$$V_{corr} = -0.6109\, r_s^{-\frac{1}{2}} (-0.0081 + 1.127\tau^2 + 2.756\tau^4) \times (1.0 + 1.291\tau^2 + 3.593\tau^4)^{-1} \tanh(\tau^{-\frac{1}{2}}), \tag{11}$$

$$\tau = 2\left(\frac{4}{9\pi}\right)^{\frac{2}{3}} r_s^2\, k_B\, T,$$

$$r_s^{-1} = \left(\frac{4}{3}\pi n_e\right)^{\frac{1}{3}}.$$

In practice, the integral in (5) is replaced by a summation and an 8-point Gaussian quadrature was used to evaluate ρ_e for each value of r. At large distances, the convergence of the sum over partial waves in (5) is rather slow and we found it necessary to include up to 50 or 70 partial waves, depending on the value of k, to achieve sufficient accuracy for $r < r_o$.

The effect of Fermi degeneracy is taken into account by the distribution function W(k) in (5) for densities equal to ρ_∞. For the cases studied in this paper the Fermi degeneracy causes only minor deviations from the Maxwell-Boltzmann distribuiton. Inside the boundary r_o, where the plasma electrons in our model are described by wave functions and where the local electron densities may reach values substantially larger than ρ_∞, the effect of degeneracy should be properly taken into account by using an antisymmetric function for the whole system. Due to complications arising from this procedure, we have ignored the possible additional effects of Fermi degeneracy inside r_o. Also all effects due to relativistic corrections have been ignored since they are probably negligible for light nuclei.

Radial functions $P_{n\ell}$ of the bound electron satisfy the equation

$$\left[\frac{d^2}{dr^2} - \frac{\ell(\ell+1)}{r^2} + 2V_b(r) + 2E_{n\ell}\right] P_{n\ell}(r) = 0. \tag{12}$$

The potential V_b acting on the bound electron is given by (2) with $\rho_b = 0$. The energy shift of a hydrogenic level $n\ell$ due to the plasma polarization is

$$\Delta E_{n\ell} = E_{n\ell} + Z^2(2n^2)^{-1} \quad . \tag{13}$$

Equations (1), (2), (4), (5), (8) and (12) should be solved self-consistently with the boundary condition

$$rV(r) \to 0, \; P_{n\ell}(r) \to 0 \tag{14}$$

for $r \to \infty$. In practice this condition should be satisfied at $r = r_o$.

The equations were solved iteratively starting with hydrogenic $P_{n\ell}$ (for hydrogenic ions) and with V(r) initially replaced by a Debye-Huckel potential. First we found a self-consistent potential (2) while keeping $P_{n\ell}$ unchanged. This procedure requires up to four iterations. Then we used the new form of $P_{n\ell}$ obtained from (12) for the following sequence of iterations. It was found that in all cases presently studied the second sequence of iterations did not lead to any substantial improvement of results and that the first sequence already yielded self-consistent values of $P_{n\ell}$ and $E_{n\ell}$.

III. RESULTS FOR Ne^{+10}, Ne^{+9} and Ar^{+17}

Figure 1 shows two typical examples of the quantity rV for Ne^{+10}, where V is the self-consistent potential (2) with $\rho_b = 0$. These results are compared with the Debye-Huckel theory of plasma screening, which agrees well with the self-consistent potential at distances larger than 2D, where D is the Debye screening length, but the Debye-Huckel potential is systematically lower in the inner region. The difference appears to increase with decreasing values of D.

The calculations for hydrogen-like Ne^{+9} and Ar^{+17} were performed with the simplifying assumption that the levels 1s, 2s and 2p are populated according to Boltzmann statistics and that all occupation numbers $b_{n\ell}$ with $n > 2$ are zero. The local densities $n_e(r)$ and $n_p(r)$ of free electrons and protons for $N_e = 3 \times 10^{24}$ cm^{-3} and T = 200 eV are displayed on Figs. 2 and 3 for Ne^{+9}. The oscillatory behavior of n_e is caused by interference effects and is mainly due to the slowly moving electrons.

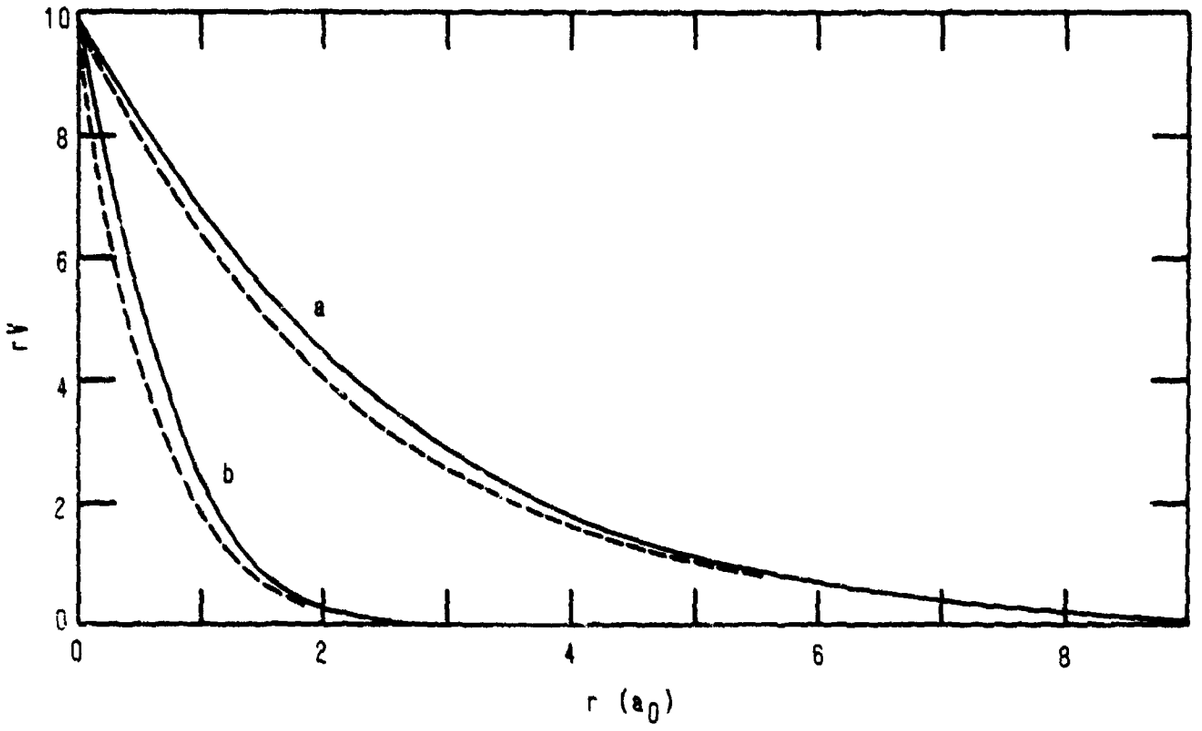

Figure 1. The quantity rV for Ne^{+10}. Full curve - present results; dashed curve - Debye-Huckel theory.
a - $N_e = 10^{24}$, T = 500 eV; b - $N_e = 6 \times 10^{24}$, T = 200 eV.

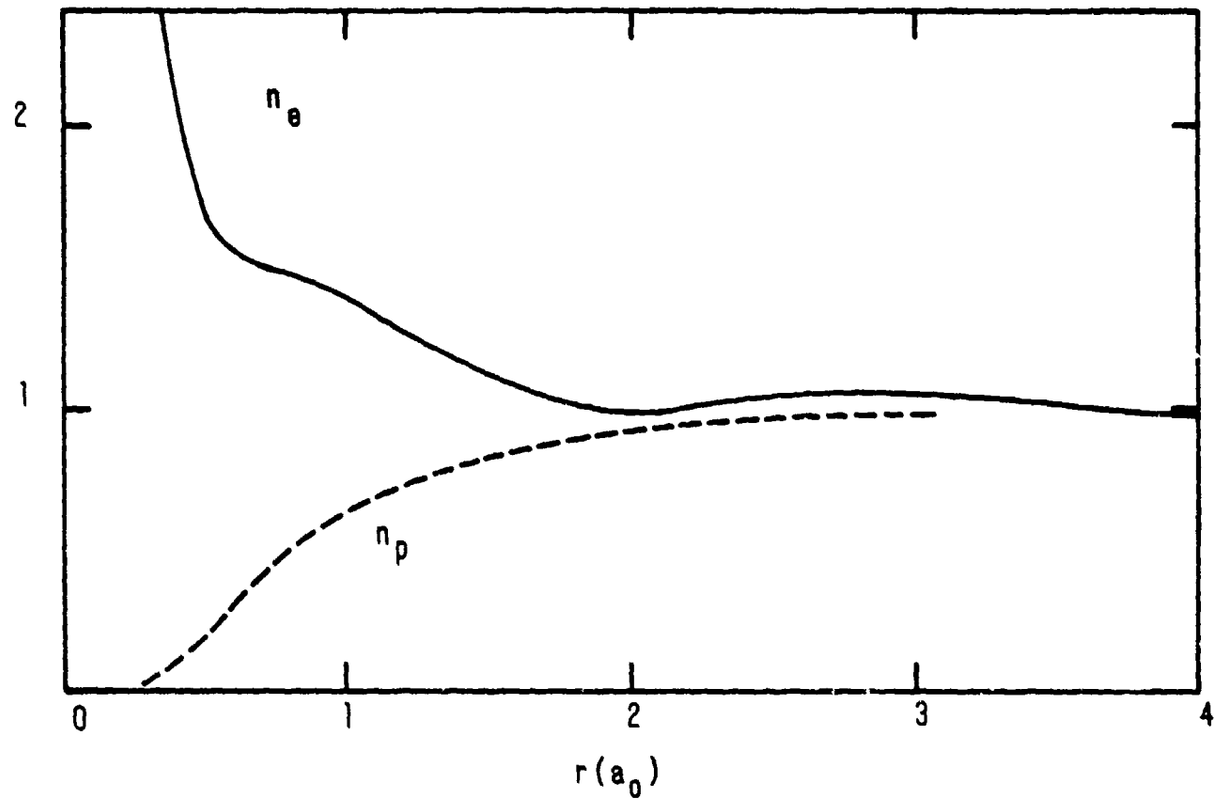

Figure 2. Density distribution of free electrons and protons for Ne^{+9}. Densities are normalized to unity at infinity. $N_e = 3 \times 10^{24}$, T = 200 eV.

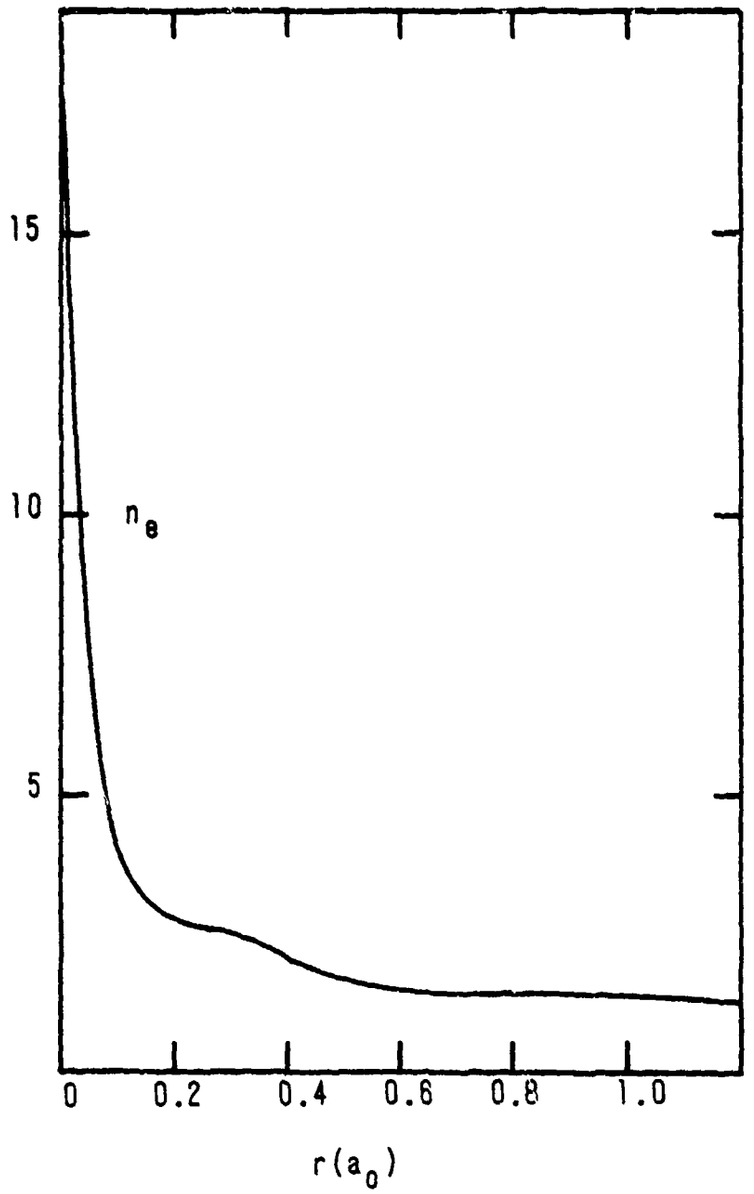

Figure 3. Same as in Figure 2.

Table 1 presents the atomic level shifts (13) for two temperatures and three electron densities N_e. Resulting line shifts of the Lyman α radiation are shown in Figs. 4 and 5. The line shifts are assumed to be equal to the difference of level shifts. The present values of line shifts are slightly larger than the results of Skupsky[6] who treated the free electrons classically with quantum mechanical corrections to the potential.

Table 2 shows how the Einstein coefficients of transition probability A for the Lyman α line are affected by plasma conditions. A_{Coul} is the coefficient corresponding to the pure Coulomb field, i.e. to $N_e = 0$. The change of transition probabilities is a consequence of the line shift combined with the change of radial functions $P_{n\ell}$. In order to ascertain the sensitivity of line shifts to the choice of $b_{n\ell}$, we carried out additional calculations for Ne^{+9} with the assumption that only the 1s ground level is occupied. The resulting line shifts were found to be only about 1% smaller than those shown in Fig. 4.

In the present calculations we have ignored all effects related to the time dependent perturbations by plasma electrons and protons. In particular, a possible redistribution of electron velocities inside the boundary r_o due to electron-electron and electron-proton collisions was not taken into account and effects leading to broadening of spectral lines were also omitted. Thus the results indicate the magnitude of effects caused by plasma polarization alone. In situations where there are only few electrons inside the Debye sphere and collisions do not happen very often, the present treatment should be perferable to the procedures based on statistical considerations for plasma electrons.

The calculation of collision excitation cross sections and rates in a dense plasma should proceed, in principle, along the lines of many-body quantum theory. However, the two-body approximation may still be useful not only for approximate evaluation of excitation rates, but especially because its simplicity allows us to separate various plasma effects.

The change in the value of excitation cross sections and rates in dense plasmas is the result of several causes: (a) changed excitation energy, (b) changed wave functions of atomic electrons, (c) distortion of the incident and scattered waves by the charge cloud around the target ion, (d) modification of the Coulomb interaction potential $|\vec{r}_1 - \vec{r}_2|^{-1} \equiv r_{12}^{-1}$ for the colliding and bound electron by plasma effects, and (3) other effects of many-body interactions.

Table 1

LEVEL SHIFT (eV)

	T(eV)	$N_e(cm^{-3})$	1s	2s	2p
Ne X	200	10^{24}	122.8	115.6	117.5
		$3x10^{24}$	194.0	173.3	178.5
		$6x10^{24}$	225.5	189.8	198.1
	500	10^{24}	90.0	85.5	86.7
		$3x10^{24}$	147.3	134.2	137.5
		$6x10^{24}$	199.6	174.3	180.3
Ar XVIII	1000	$2x10^{25}$	475.8	439.9	449.1
		$5x10^{25}$	702.0	616.4	637.5
		$8x10^{25}$	865.0	736.0	766.4
	2000	$2x10^{25}$	375.8	351.0	357.3
		$5x10^{25}$	563.8	504.5	518.8
		$8x10^{25}$	695.0	602.6	624.3

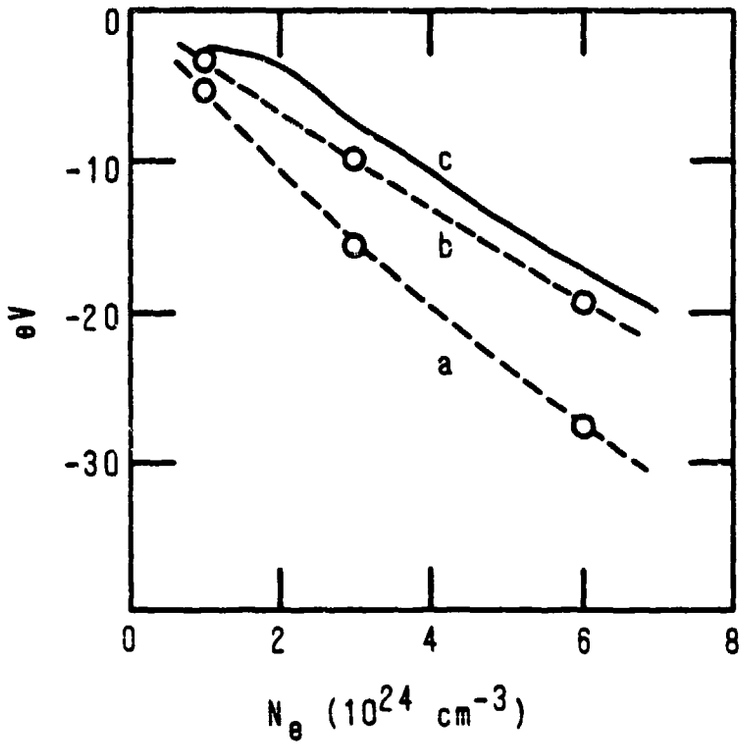

Figure 4. Density dependence of the Ne X Lyman - α line shift. a - T = 200 eV; b - T = 500 eV; c - results of Skupsky[6] (T = 500 eV).

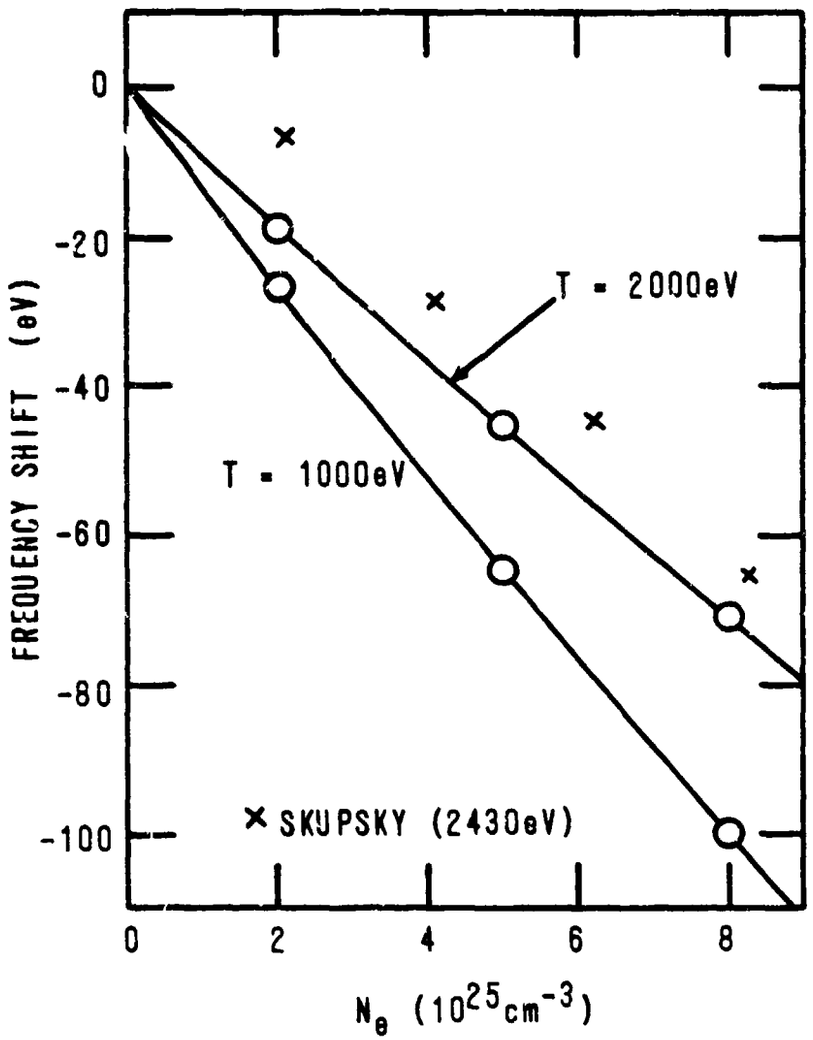

Figure 5. Density dependence of the Ar XVIII Lyman - α line shift.

Table 2

$A(2p \rightarrow 1s)/A_{Coul}\ (2p \rightarrow 1s)$

	T(eV)	N_e (cm^{-3}) 10^{24}	3×10^{24}	6×10^{24}
Ne X	200	0.967	0.904	0.840
	500	0.981	0.942	0.887
		N_e (cm^{-3}) 2×10^{25}	5×10^{25}	8×10^{25}
Ar XVIII	1000	0.950	0.879	0.816
	2000	0.967	0.919	0.873

We have calculated collision strengths for the 1s - 2s, 1s - 2p, and 2s - 2p transitions of Ne^{+9} and Ar^{+17} using the formalism of the distorted-wave method without exchange. Excitation energies and atomic wave functions were taken from our self-consistent calculations and the equation for the radial functions of the colliding electron were solved using the self-consistent potential (2). However, the modificaiton of the potential of mutual interaction r_{12}^{-1} cannot be properly described within the formalism of the distorted-wave approximation, unless the wave functions of plasma electrons take into account correlation effects between the bound and the free electrons. The variational expression for the element of the reactance matrix then contains an additional term that partially cancels the term of direct Coulomb interaction r_{12}^{-1} as a result of decreased local density of plasma electrons in the vicinity of the bound electron. One can approximate this effect by using the free electron wave functions without correlation and replacing r_{12}^{-1} in the matrix element by $r_{12}^{-1} f(r_{12})$, where $f(r_{12})$ is a properly defined screening function.

$r_{12}^{-1} f(r_{12})$ can be expanded in the form

$$r_{12}^{-1} f(r_{12}) = r_>^{-1} \sum_{\lambda=0}^{\infty} P_\lambda (\cos \omega) \sum_{\mu=0}^{\infty} A_{\lambda\mu}(r_>) (r_</r_>)^{\lambda + 2\mu}, \qquad (15)$$

where ω is the angle between $\vec{r}_1$ and $\vec{r}_2$ and the coefficients $A_{\lambda\mu}$ depend on the form of $f(r_{12})$.

To demonstrate the effect of screening of the mutual interaction, we have adopted a Debye-Huckel form of the screening function. The expansion (15) have the form

$$r_{12}^{-1} \exp(-r_{12}/D) = \left[r_>^{-1} + \frac{1}{6} (r_>/D)^2 (r_<^2/r_>^3) + \ldots \right] \exp(-r_>/D) P_o(\cos \omega)$$

$$+ \left[(1 + r_>/D) (r_</r^2) + \frac{1}{10} (1 + r_>/D) (r_>/D)^2 (r_<^3/r_>^4) + \ldots \right] \qquad (16)$$

$$\times \exp(-r_>/D) P_1 (\cos \omega) + \ldots$$

The results for selected values of T and N_e are shown on Figs. 6-11. Also

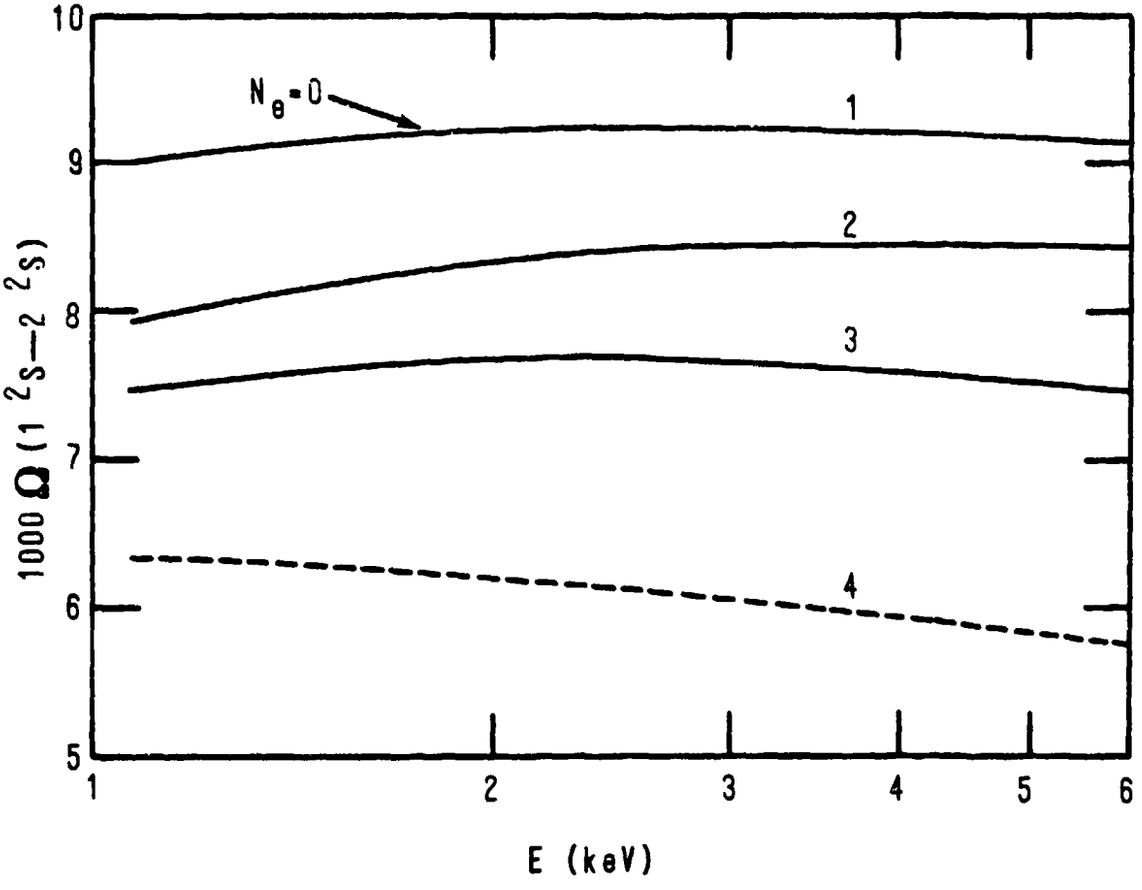

Figure 6. Collision strength Ω ($1s^2S$, $2s^2S$) for Ne^{+9}. T = 200 eV. 1 - N_e = 0; 2,3,4 - $N_e = 3 \times 10^{24}$ cm^{-3}; 2 - D = ∞; 3 - D = Λ; 4 - D = $\frac{1}{2}$ Λ (Λ - Debye length).

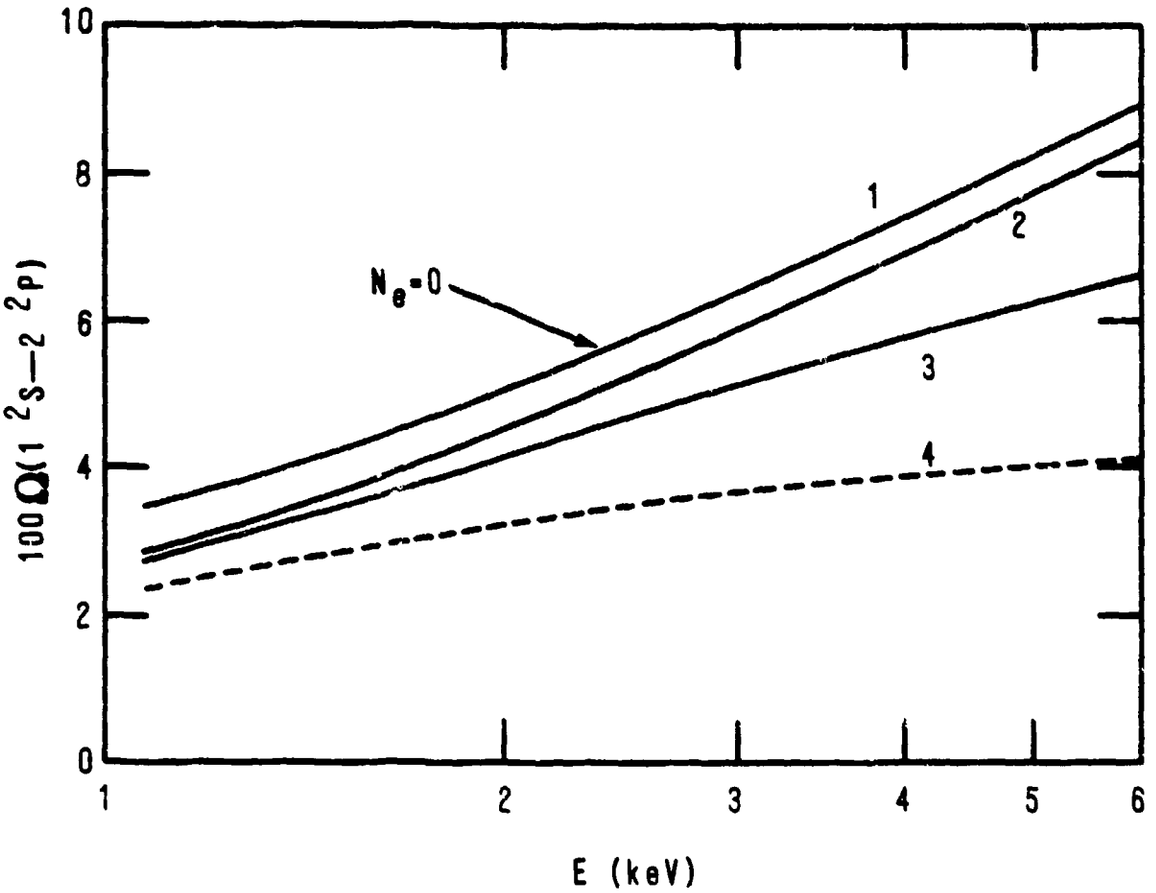

Figure 7. Collision strength Ω ($1s^2S$, $2p^2P$) for Ne^{+9}. T - 200 eV. 1 - N_e = 0; 2,3,4 - N_e = 3×10^{24} cm^{-3}; 2 - D = ∞; 3 - D = Λ; 4 - D = $\frac{1}{2}$ Λ (Λ = Debye length).

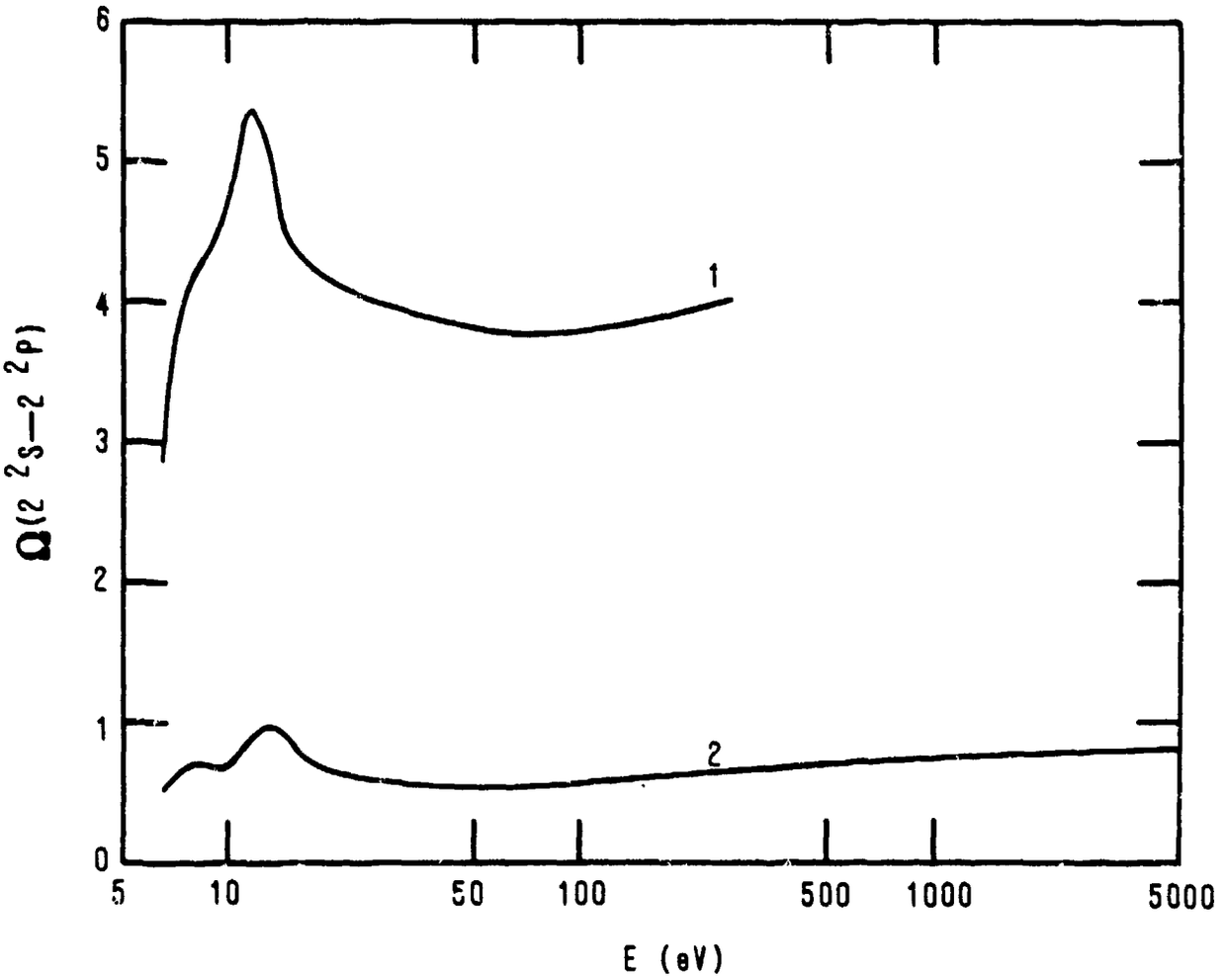

Figure 8. Collision strength Ω ($2s^2S$, $2p^2P$) for Ne^{+9}. T = 200 eV; $N_e = 3 \times 10^{24}$ cm^{-3}. 1 - D - ∞; 2 - D = Debye length.

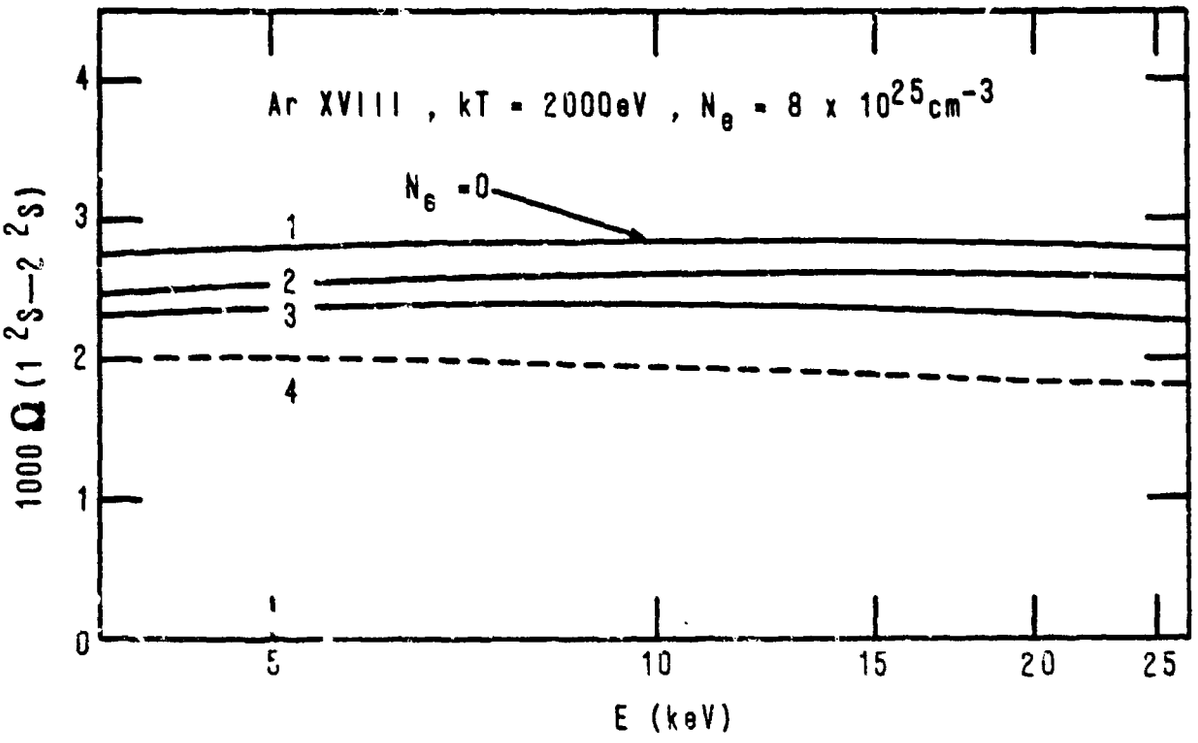

Figure 9. Collision strength Ω ($1s^2S$, $2s^2S$) for Ar^{+17}. T = 2000 eV.
1 - N_e = 0; 2,3,4 - N_e = $8x10^{25}$ cm^{-3}; 2 - D = ∞;
3 - D = Λ, 4 - D = $\frac{1}{2}$Λ (Λ - Debye length).

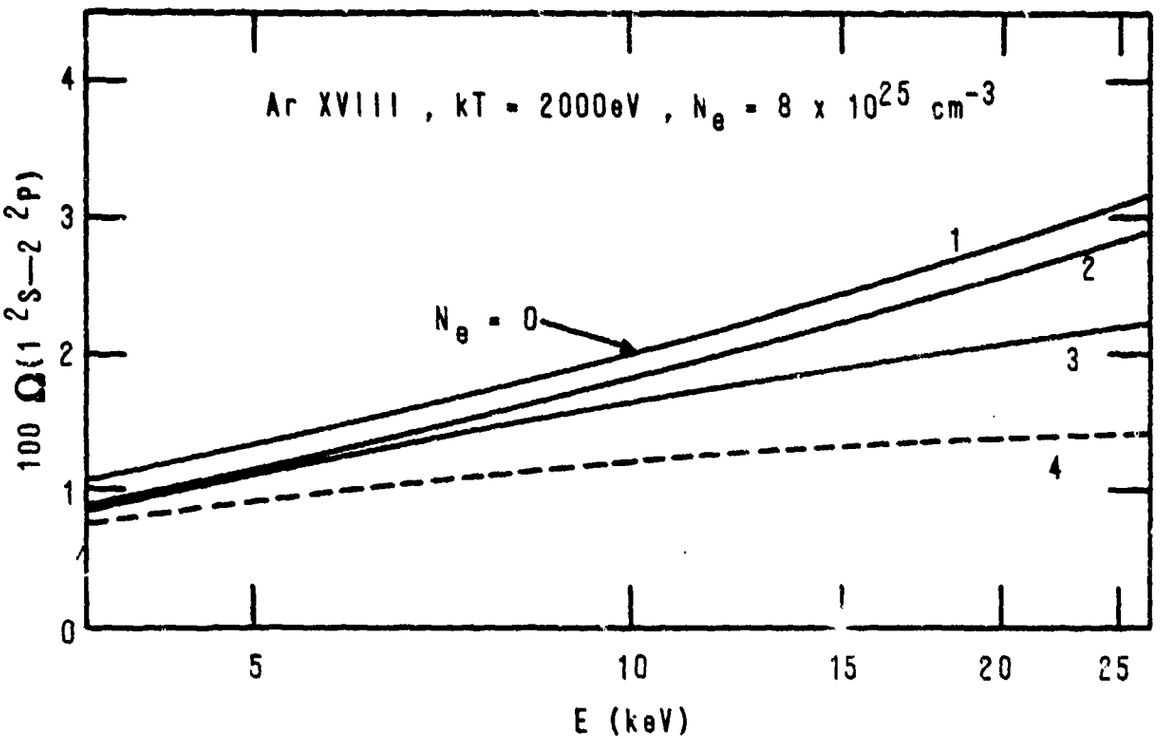

Figure 10. Collision strength Ω ($1s^2S$, $2p^2P$) for Ar^{+17}. T = 2000 eV.
1 - N_e = 0; 2,3,4 - N_e = 8 x 10^{25} cm^{-3}; 2 - D = ∞;
3 - D = Λ; 4 - D = $\frac{1}{2}$ Λ (Λ = Debye length).

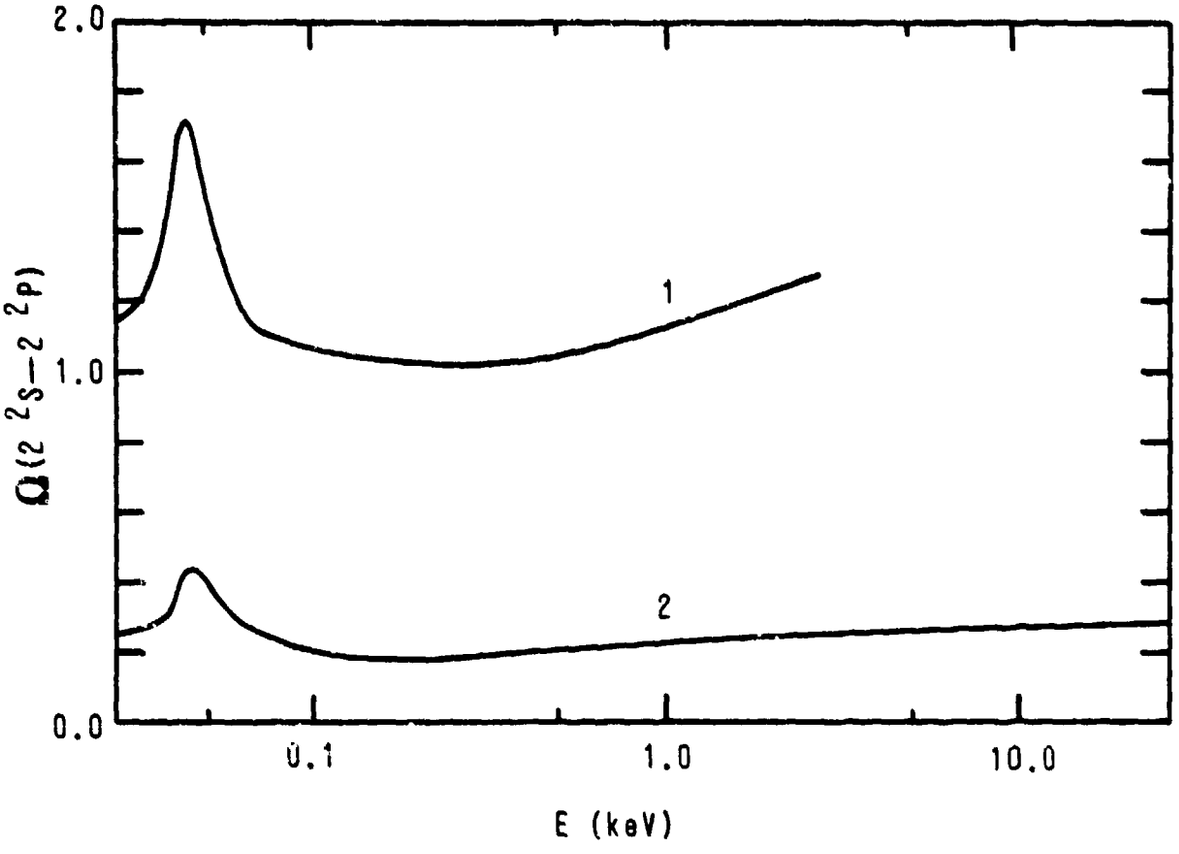

Figure 11. Collision strength Ω ($2s^2S$, $2p^2P$) for Ar^{+17}. T = 2000 eV; $N_e = 8x10^{25}$ cm^{-3}. 1 - D = ∞; 2 - D = Debye length.

shown are the collision strengths without any plasma effects ($N_e = 0$) for the transitions 1s - 2s, 1s - 2p. The change of atomic wave functions by plasma polarization has a very small effect on the cross sections for conditions considered in this investigation. The change of excitation energies produces a negligible effect on the 1s - 2s and 1s - 2p transitions but it removes the degeneracy of the 2s and 2p levels and reduces the 2s - 2p cross sections to finite values. For the 1s - 2s and 1s - 2p transitions, calculations were made for 3 values of the screening parameter D in (16). $D = \infty$ corresponds to the situation where the modification of mutual interaction is ignored and the lowering of the collision strength is caused only by the defocusing of colliding electrons (curve 2 on Figs. 6, 7, 9, 10). Curves 3 and 4 were obtained with $D = \Lambda$ and $D = 1/2\ \Lambda$, where Λ is the Debye length for the corresponding temperature and density.

The effect of screening on partial collision strengths increases with increasing angular momentum (Fig. 12) and therefore the dipole transition 1s - 2p is more affected than the monopole transition 1s - 2s. The term corresponding to $\mu = 1$ in the expression (15) and (16) has only a very small effect on the collision strengths.

Collisions strengths for the 2s - 2p transition were calculated for $D = \infty$ and $D = \Lambda$. The sensitivity of Ω to the value of D is much greater than for the 1s - 2s and 1s - 2p transitions, because the excitation energy is much smaller, many more partial waves contribute to Ω at a given energy and higher angular momenta are more affected by screening. Collision strengths exhibit a resonance-like behavior in the low-energy region above the excitation threshold. The enhancement of Ω is caused almost exclusively by the contribution from the $\ell = 2,3$ incident partial waves in Ne^{+9} and by $\ell = 3$ in Ar^{+17}.

IV. RESULTS FOR HYDROGEN AND IONIZED HELIUM

At the present time, there are no experimental data that could be compared with the theoretical results for Ne^{+9} and Ar^{+17}. Therefore we have extended the calculations to neutral hydrogen and singly ionized helium which have been studied experimentally. Unfortunately, the measurement of plasma polarization shifts is a difficult problem and results of various experiments do not always agree with each other. Moreover, the measured shifts represent

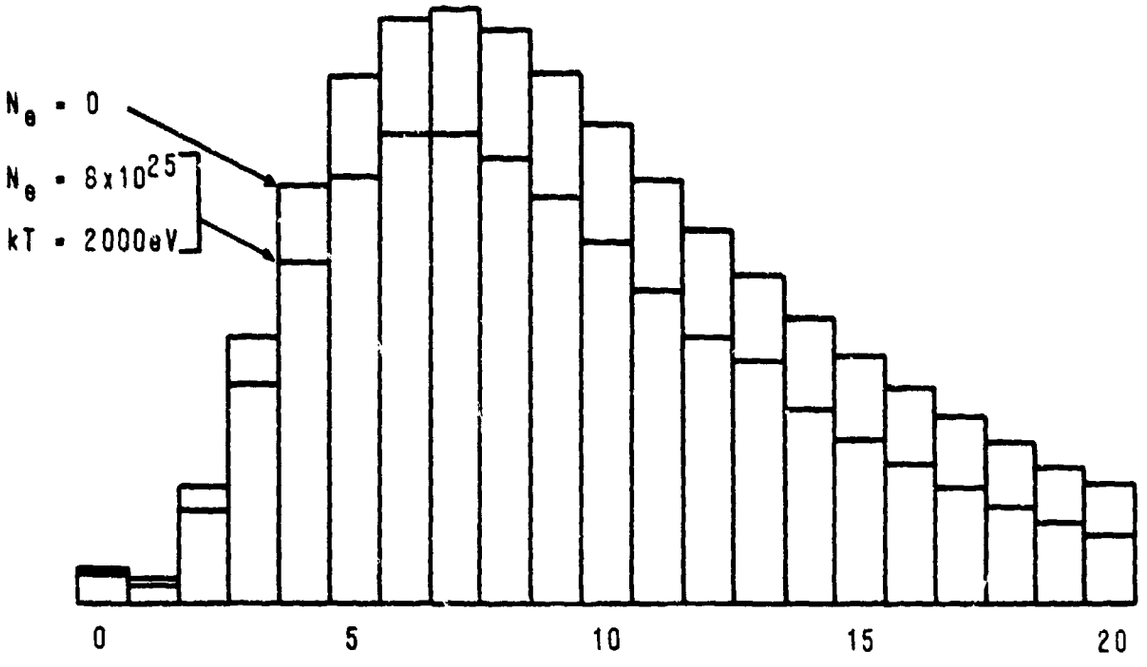

Figure 12. Comparison of partial contributions to the collision strength Ω ($1s^2S$, $2p^2P$) for Ar^{+17} for $N_e = 0$ and $N_e = 8 \times 10^{25}$ cm^{-3}, T = 2000 eV, D = Å.

a combined effect of plasma polarization (i.e. space charges around the atom), ion quadrupole shifts, quadratic Stark effect and shift arising from electron collisions. These additional effects have been ignored in our present investigation and therefore our results for H and He^+ have only a qualitative character.

The plasma conditions in which neutral hydrogen and ionized helium radiate correspond to such low electron densities ($\lesssim 10^{17}$ cm^{-3}) that several substantial simplications in our theoretical treatment are possible. In the limit of low charge density (due to plasma electrons and positive ions in the vicinity of the radiating atom) we may omit the effect of these space charges on the motion of free electrons and we solve eq. (8) with $V_{ex} = V_{corr} = 0$ and with V from (2) with $\rho_e = \rho_p = 0$. ρ_b is again given by (1), but due to the low temperature, the population of excited levels is so small that it may be omitted altogether.

We will consider pure hydrogen and pure helium plasma and for the sake of simplicity we will assume that the fraction of doubly ionized helium ions is very small. Then all positive ions are singly ionized and we may replace ρ_p by ρ_i in eq. (2) - (4). For the positive charge distribution we again adopt eq. (4) and in order to demonstrate the effect of different ion distributions on level shifts we use three different forms of V: (a) V = 0 which corresponds to a uniform ion distribution, (b) V calculated from (2) with $\rho_e = \rho_p = 0$ and with ρ_b from (1) assuming that only the 1s level is occupied. (c) V from (2) with $\rho_e = \rho_p = 0$ and ρ_b from (1) assuming that only the level $n\ell$, for which the shift is being calculated, is occupied. This last choice may find a justification if we compare de Broglie wavelength λ_B for thermal electrons and ions: while λ_B for electrons is comparable or larger than the dimensions of the atom and therefore plasma electrons do not adjust to individual atomic states $n\ell$, λ_B for ions is much smaller and the ion distribution may depend on $n\ell$. In using eq. (4) for the ion distribution, one should employ, of course, the true interatomic potential V. This potential may be substantially different, especially for hydrogen, from the potential we are using the present work. This is another reason why out results should be compared with experiment only with caution.

The level shifts in the low-density limit are calculated from the perturbation expression

$$\Delta E_{n\ell} = -\int_0^\infty P_{n\ell}^2 \; V' \; dr, \tag{17}$$

where $V' = V - Zr^{-1}$ and V is calculated from (2) with $\rho_b = 0$, $\rho_p = \rho_i$ and with ρ_i and ρ_e obtained by the procedure just described. In the low-density limit we do not perform self-consistent calculations and therefore we do not know the correct behavior of V at large distances. Consequently we cannot carry out the integration in (17) up to the indicated upper limit and cannot calculate absolute level shifts as in the high density case. However, we can obtain relative shifts $\Delta E_{n\ell} - \Delta E_{n'\ell'}$ if we integrate, in (17), up to the distance beyond which all radial functions $P_{n\ell}$ involved in the calculation vanish.

From (17) it follows that level shifts are proportional to electron density N_e. As a consequence, we do not have to perform a thermal average of electron density distribution before calculating the potential from (2) and shifts from (17), but instead we can first calculate shifts for the charge distribution corresponding to a given velocity of electrons and perform the thermal average of these shifts. They are a smooth function of electron velocity and the average can be obtained with great accuracy.

We have obtained relative level shifts for all $n\ell$ levels of H and He^+ with n - 1 to 4. Weighted averages over the ℓ - values for each principal quantum number n, normalized to the density $N_e = 10^{17}$ cm^{-3} are displayed on Figs. 13 and 14. Relative level shifts for H are more sensitive to the choice of the ion distribution than for He^+.

For He^+, our results predict a very small red shift of Lyman series lines. The experimental evidence, however, points to a much larger blue shift[2]. Theoretical blue shifts were derived by Greig et al.[9], Burgess and Peacock[10] and Volonté[11], but the apparent agreement of all these theoretical results with experiment is basically due to the omission of space charges outside the orbit of the bound electron, and this assumption does not appear to be properly justified.

For the 3 - 2 transition of He^+ at 1640 Å our theory predicts a negligible red shift in agreement with experiment, but the theoretical shift for the 4 - 2 transition at 1215 Å is again too small, except possibly for the temperature around 4 eV.

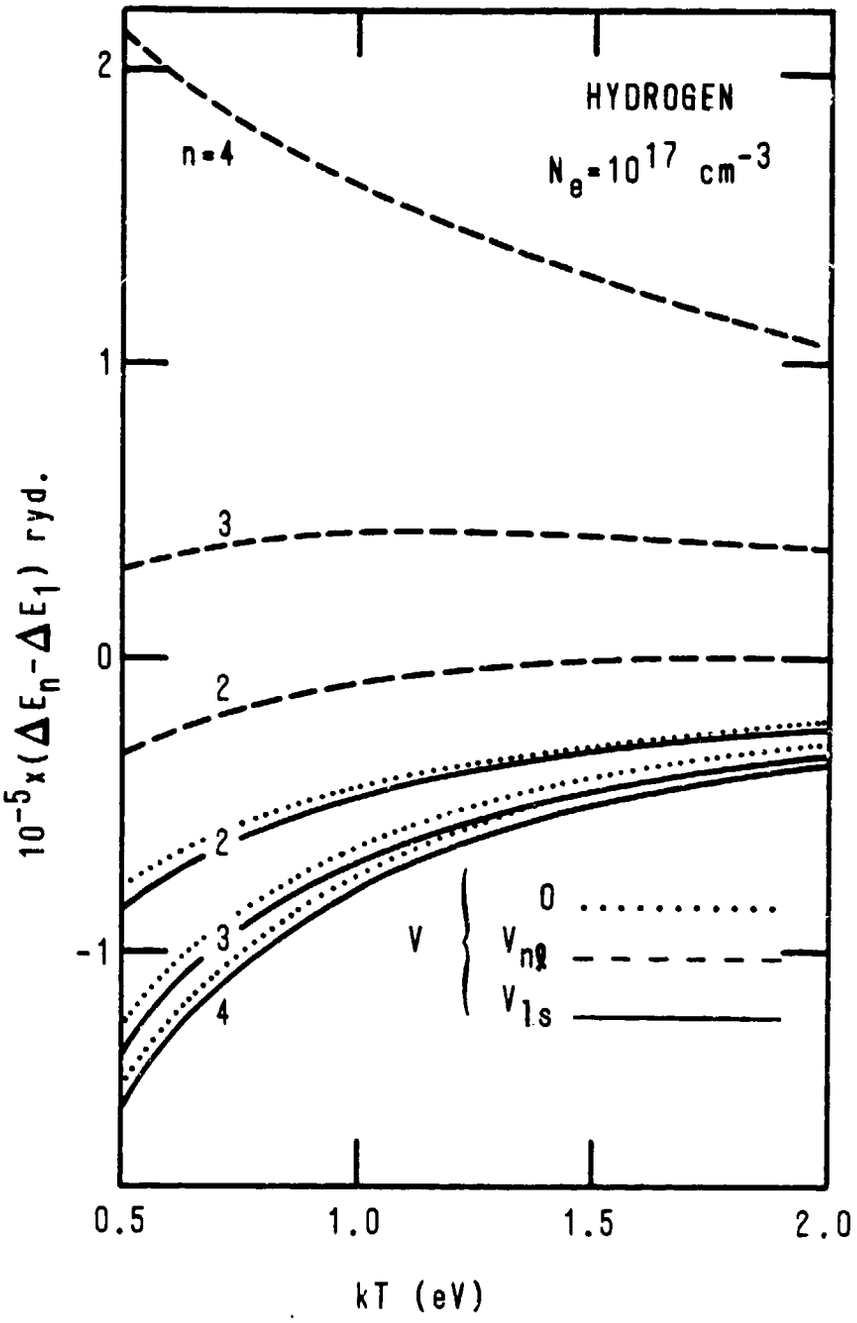

Figure 13. Temperature dependence of relative level shifts for hydrogen. Dotted lines: uniform ion distribution (ion density obtained form eq. (4) with V=0). Broken lines: ion density given by eq. (4) with V derived from screening by the nℓ electron. Solid line: ion density given by eq. (4) with V derived from screening by the 1s electron.

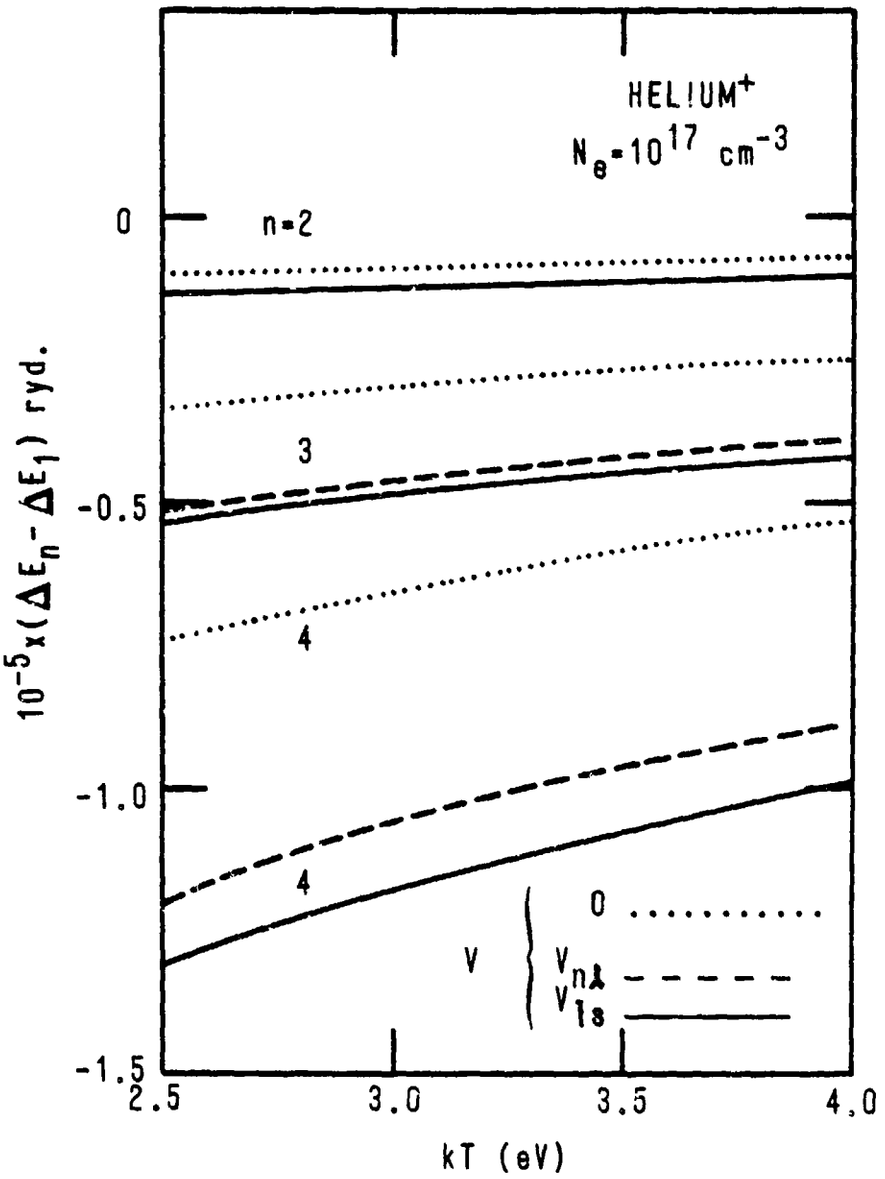

Figure 14. Temperature dependence of relative level shifts for helium$^+$ Dotted lines: uniform ion distribution (ion density obtained form eq. (4) with V=0). Broken lines: ion density given by eq. (4) with V derived from screening by the nℓ electron. Solid line: ion density given by eq. (4) with V derived from screening by the 1s electron.

Pittman et al.[12] measured a red shift of 0.17 Å for the transition 4 - 3 at 4686 Å for T = 4 eV . . . + From Fig. 14 we find shifts of 0.07, 0.12 and 0.14 Å for three different ion distributions. This may be considered a satisfactory agreement with respect to the uncertainty of the ion distribution.

The same authors also measured red shifts of the Balmer series lines of neutral hydrogen. Our theoretical results predict either much smaller values or even blue shifts, but an agreement can hardly be expected due to the very approximate form of the ion distribution.

For reasons mentioned earlier, the comparison with experiment is generally very inconclusive. The theoretical treatment should be improved first of all by using correct ion distribution and by properly taking into account other effects leading to the shifts of atomic levels.

ACKNOWLEDGMENT

This work was supported, in part, by the Office of Naval Research and NASA. We would also like to acknowledge useful discussions with Drs. H. R. Griem and M. W. C. Dharma-wardana.

REFERENCES

1. H. R. Griem, Proc. 7th Int. Conf. on Phenomena in Ionized Gases, Belgrade, Yugoslavia (1965).
2. M. Neiger and H. R. Griem, Phys. Rev. A 14, 291 (1976).
3. J. R. Van Zandt, J. C. Adcock, and H. R. Griem, Phys. Rev. A 14, 2126 (1976).
4. O. Theimer and P. Kepple, Phys. Rev. A 1, 957 (1970).
5. B. F. Rozsnyai, J. Quant. Spectrosc. Radiat. Transfer 15, 695 (1975); Phys. Rev. A 5, 1137 (1972).
6. S. Skupsky, Phys. Rev. A 21, 1316 (1980).
7. M.W.C. Dharma-wardana, private communication (1980).
8. M.W.C. Dharma-wardana and R. Taylor, J. Phys. C: Solid St. Phys. 13, XXX (1980).
9. J. R. Greig, H. R. Griem, L. A. Jones, and T. Oda, Phys. Rev. Lett. 24, 3 (1970).
10. D. D. Burgess and N. J. Peacock, J. Phys. B4, L94 (1971).
11. S. Volonté, J. Phys. B8, 1170 (1975).
12. T. L. Pittman, P. Voigt, and D. E. Kelleher, Phys. Rev. Lett. 45, 723 (1980).

DISTRIBUTION LIST

David D. Burgess
The Blackett Laboratory
Imperial College
London SW7 2BZ
England

Chander P. Bhalla
Physics Department
Kansas State University
Manhattan, Kansas 66506

J. Cooper
JILA
University of Colorado
Boulder, Colorado 80302

T. R. Carson
University Observatory
St. Andrews
Fife, Scotland
UK KY16 9LZ

George F. Chapline
Lawrence Livermore National Laboratory
P.O. Box 808 L-71
Livermore, California 94550

Raju U. Datla
National Bureau of Standards
Building 221
Washington, D.C. 20234

Richard J. Fortner
Lawrence Livermore National Laboratory
P.O. Box 808 L-401
Livermore, California 94550

Amnon Fisher
Department of Physics
University of California
Irvine, California 92717

A. H. Gabriel
Space and Astrophysics Division
Appleton Laboratory
Chilton, Didcot, Oxon.
OX11 00X, United Kingdom

Harold C. Graboske, Jr.
Lawrence Livermore National Lab.
P. O. Box 808 L-355
Livermore, California 94550

Alan Hauer
M.S. 554
Los Alamos National Laboratory
P. O. Box 1663
Los Alamos, New Mexico 87545

Walter F. Heubner
M. S. 212
Los Alamos National Laboratory
P. O. Box 1663
Los Alamos, New Mexico 87545

Alan L. Hoffman
Mathematical Sciences Northwest
P. O. Box 1887
Belevue, Washington 98009

Frank E. Irons
Western Mining Corporation
55 MacDonald Street
Kalgoorlie, 6430
Western Australia

Lawrence A. Jones
M.S. 455
Los Alamos National Laboratory
P. O. Box 1663
Los Alamos, New Mexico 87545

Elisabeth Kallne
Dept. of Physics
University of Virginia
Charlottesville, Va. 22901

Joseph D. Kilkenny
The Blackett Laboratory
Imperial College
London SW7 2BZ
England

Kenneth W. Hill
Plasma Physics Laboratory
Princeton University
Princeton, New Jersey 08540

Hans-Joach I. Kunze
Inst. Experimentalphysik
Ruhr Universitat
Postfach 2148
4630 Bochum
West Germany

Richard W. Lee
The Blackett Laboratory
Imperial College
London SW7 2BZ
England

James G. Lunney
Department of Physics
Queen's University of Belfast
Belfast, Northern Ireland
United Kingdom

Eugene J. McGuire
Org. 4211
Sandia Laboratories
Albuquerque, New Mexico 87185

Richard M. More
Lawrence Livermore National Laboratory
P. O. Box 808 L-355
Livermore, California 94550

Carl Moser
Centre Europeande Calcul Atomique
et Moleculaire
Batiment 506
Universite de Paris XI
91405 Orsay Cedex
France

Dennis L. Matthews
Lawrence Livermore National Laboratory
P. O. Box 808 L-313
Livermore, California 94550

Joseph D. Perez
Lockheed Palo Alto Research Lab.
3251 Hanover Street (5211)
Palo Alto, California 94304

G. J. Pert
Dept. of Applied Physics
University of Hull
Hull HU6 7RX
England, United Kingdom

N. J. Peacock
UKAEA
Culham University
Abingdon, Oxon
OX 143DB, United Kingdom

Jay Pearlman
Maxwell Laboratories
8835 Balboa Avenue
San Diego, California 92123

A. K. Rajagopal
Dept. of Physics and Astronomy
Louisiana State University
Baton Rouge, Louisiana 70803

Balazs F. Rozsnyai
Lawrence Livermore National Laboratory
P. O. Box 808 L-71
Livermore, California 94550

Michael Stroscio
AFOSR/NP
Bolling Air Force Base
Washington, D.C. 20332

Stanley Skupsky
Laboratory for Laser Energetics
University of Rochester
250 E. River Road
Rochester, New York 14623

David Salzmann
Soreq Nuclear Research Center
Yavne 70600
Israel

C. Bruce Tarter
Lawrence Livermore National Laboratory
P. O. Box 808 L-71
Livermore, California 94550

Jon C. Weisheit
Plasma Physics Laboratory
Princeton University
P. O. Box 451
Princeton, New Jersey 08544

Wolfgang Wiese
National Bureau of Standards
Rm. A267, Bldg. 221
Washington, D.C. 20234

David M. Woodall
Dept. of Nuclear Engineering
University of New Mexico
Albuquerque, New Mexico 87131

Barukh Yaakobi
Laboratory for Laser Energetics
University of Rochester
250 E. River Road
Rochester, New York 14623

Zev Zinamon
The Weizmann Institute of Science
Rehovot, Israel

Norman Rostoker
Dept. of Physics
University of California
Irvine, California 92717

Alan Kolb
Maxwell Laboratories
8835 Balboa Avenue
San Diego, Calif. 92123

Alan Merts
Los Alamos National Scientific Lab.
P. O. Box 1663
Los Alamos, New Mexico 87545

D. E. Kelleker
National Bureau of Standard
Washington, D.C. 20234

H. W. Drawin
EURATOM-CEA
Dept. of Plasma Physics
Center for Nuclear Study
F-92260 Fonteney-aux-Roses
France

C. F. Hooper
Dept. of Physics
Univ. of Florida
Gainesville, Florida 32611

John D. Hey
Dept. of Physics
Univ. of Cape Town
Rondebosch 7700
South Africa

G. Peach
Dept. of Physics & Astronomy
University College
Gower Street
London WCIE 6BT
England

Naval Research Laboratory
Code 4700 - 26 Copies
Code 4720 - 50 Copies